

Molecular Turnstiles Regulated by Metal Ions

Guangxia Wang,^{†,‡,§} Hongmei Xiao,[†] Jiaojiao He,[†] Junfeng Xiang,[‡] Ying Wang,^{*,†} Xuebo Chen,^{*,†} Yanke Che,^{*,‡} and Hua Jiang^{*,†}

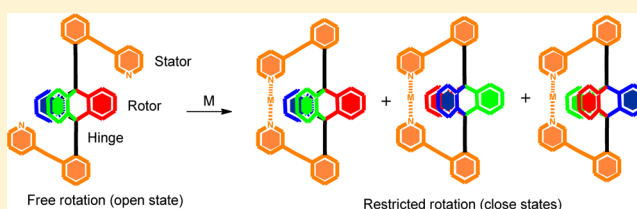
[†]Key Laboratory of Theoretical and Computational Photochemistry, Key Laboratory of Radiopharmaceuticals, Ministry of Education, College of Chemistry, Beijing Normal University, Beijing 100875, China

[‡]Beijing National Laboratory for Molecular Sciences, CAS Key Laboratory of Photochemistry, Institute of Chemistry, Chinese Academy of Sciences, Beijing 100190, China

[§]University of Chinese Academy of Sciences, Beijing 100049, China

Supporting Information

ABSTRACT: A family of novel molecular turnstiles 1–3 composed of two stators with pyridyl binding sites and a different-sized triptycene rotor was synthesized. The molecular turnstiles behave in an open state at room temperature in the absence of metal ions but display significantly different closed states in the presence of Ag⁺ and Pd²⁺. The Ag⁺-mediated turnstiles 1–3Ag exhibited closed states but unreadable bistability at ambient temperature because the Ag⁺-mediated macrocyclic framework is not able to restrict the rotations of the rotors; while temperature was decreased, the macrocyclic frameworks became stable enough to halt the rotations of the rotors, eventually leading to the readable closed states for 1–3Ag. In contrast, Pd²⁺-mediated macrocyclic frameworks are stable, giving rise to a detectable closed state of turnstiles 1–3Pd in a wide range of temperatures. These findings have also been supported by DFT calculations.



INTRODUCTION

Inspired by biomolecules such as myosin and ATP synthase capable of moving linearly or rotatively to perform required tasks, chemists have devoted much effort to develop artificial architectures constructed with (non)covalent bonds to mimic motion of its natural counterparts at the molecular level. Such devotions have led to an enormous development in synthetic molecular machinery.¹ To date, many excellent examples of functional molecular devices, including molecular shuttles,² molecular rotors,³ molecular switches,⁴ molecular gyroscopes,⁵ and molecular turnstiles,⁶ have been reported for their abilities to control movements at the molecular level and to perform tasks, for example, supramolecular catalysis.^{4b,7} Among those systems, a molecular turnstile, a rotary molecular system mainly consisting of a stator and a rotor, displays a detectable state of bistability (an open and closed state), which provides a basis for future design of functional molecular devices to perform specific tasks such as manipulation at the nanoscale and information storage.

One of the earliest examples of molecular turnstiles was reported by Moore.^{6a} The molecular turnstile, composed of a hexa(phenylacetylene) macrocyclic framework serving as a stator and a diethynylarene bridge inside the macrocycle serving as a rotor, exhibits readable but uncontrollable bistability only when the size of the rotor matches that of the macrocycle. Recently, Hosseini⁸ described a series of molecular turnstiles based on porphyrins or Pt(II) organometallic backbones, in which a switchable process between an open and a closed state was realized by modulating the metal binding

interactions between the stator and the rotor. Despite some progress made so far, molecular turnstiles are still less developed in comparison with other molecular devices, and there are still many challenges, including the efficient synthesis of a macrocyclic framework and control of the form of bistability and unidirectional rotary movement, that deserve more attention and effort in the coming years.

We envisaged a self-assembly strategy based on noncovalent forces that would provide an efficient solution for some of these problems. Metal coordinative binding, one of the noncovalent forces, displays promise for constructing functional molecular devices, as exemplified by numerous elegant supramolecular systems on silver-mediated molecular rotary systems,⁹ helicates,¹⁰ and cages.¹¹ In this contribution, we describe our self-assembly strategy for constructing novel molecular turnstiles and for regulating their bistability between an open and a closed form with metal ions as our continuous effort on functional molecular devices.¹²

As shown in Figure 1a, the molecular turnstiles consist of two stator parts with metal binding sites, a rotor part, and hinges. In the absence of a metal ion, the rotor rotates unhindered, and the turnstile behaves in an open state. In the presence of a metal ion, two stator parts are bridged by metal coordinative binding to give rise to a rigid framework, acting as a stator that should restrict the rotary motion of the rotor through steric interaction between the stator and the rotor if the size of the

Received: March 3, 2016

Published: March 17, 2016

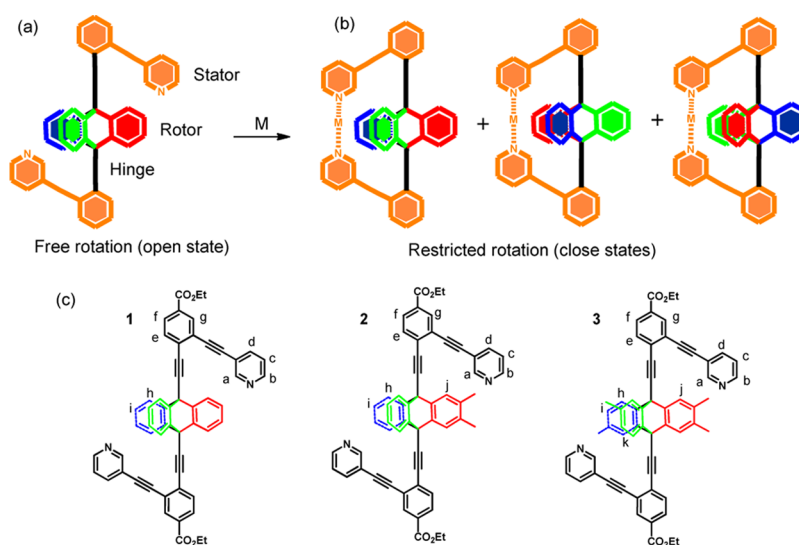
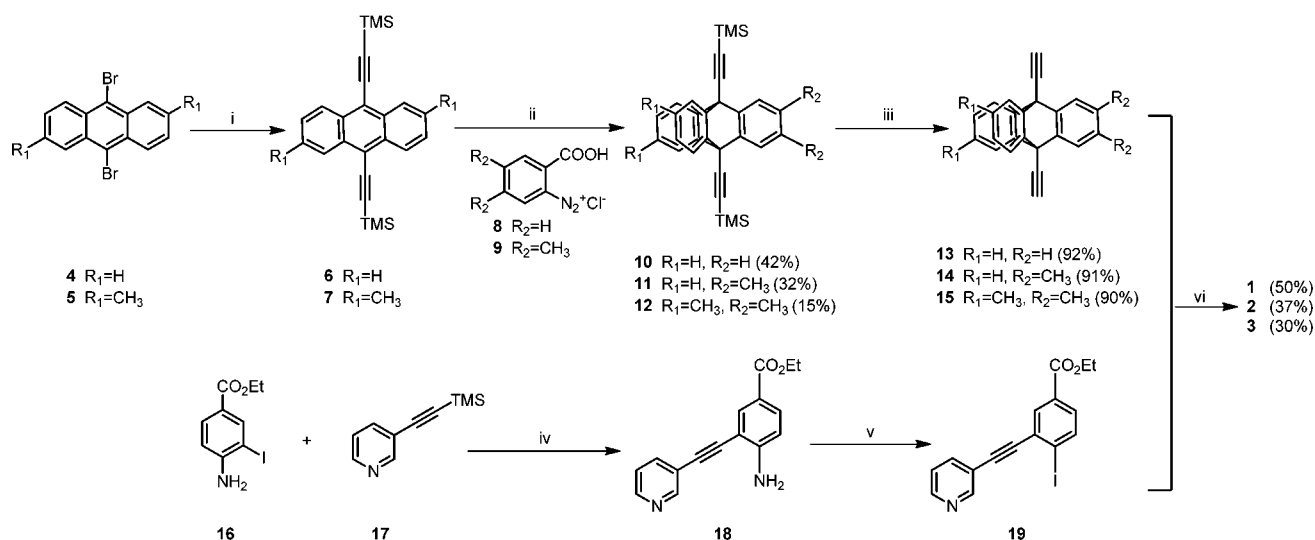


Figure 1. Schematic representation of the states of bistability in a molecular turnstile regulated by a metal ion: (a) open state; (b) closed states mediated by metal ions, with three possible homomeric rotamers of the molecular turnstiles when the phenyl groups on the rotor are differentiable (shown in different colors). In each rotamer, the rigid framework (stator) is located between the two phenyl groups. (c) Structures of molecular turnstiles 1–3 studied herein.

Scheme 1. Synthesis of Molecular Turnstiles 1–3^a



^aReagents and conditions: (i) $(Ph_3P)_2PdCl_2$, CuI, $i-Pr_2NH$, THF, TMS-acetylene; (ii) 1,2-epoxypropane, CH_2ClCH_2Cl , reflux; (iii) K_2CO_3 , THF, CH_3OH ; (iv) TBAF, $(Ph_3P)_2PdCl_2$, CuI, $i-Pr_2NH$, THF; (v) $NaNO_2$, HCl, KI; (vi) $(Ph_3P)_2PdCl_2$, CuI, $i-Pr_2NH$, THF.

rotor is larger than the stator framework and, consequently, should give rise to a closed state with up to three rotamers if the phenyl rings on the rotor are differentiable (Figure 1b). To demonstrate this proof-of-concept, we designed novel molecular turnstiles 1–3 (Figure 1c), in which two monodentate pyridyl ligands each bearing a coordinative binding site were chosen as two stator parts, and triptycyl (Tp) groups with different substituents were chosen as a rotor because of its structural uniqueness. Moreover, a Tp group or its derivative was successfully used to construct many functional molecular devices, such as molecular gears,¹³ molecular brakes,¹⁴ molecular gates,¹⁵ and rotary catenanes.¹⁶ Acetylenyl groups act as hinges to link the stator parts and the rotor together to generate a rigid framework. Ag^+ and Pd^{2+} metal ions that are inclined to adopt a linear coordination geometry¹⁷ bring two pyridyl ligands on the stator parts together to form a rigid

macrocyclic framework, which consequently leads to a closed state. We notably show that the forms of bistability of molecular turnstiles regulated by Ag^+ and Pd^{2+} through a self-assembly process are highly dependent on the binding nature of coordinative metal ions and the surrounding temperature but independent of the size of the Tp rotor itself in the present system.

RESULTS AND DISCUSSION

Synthesis. The syntheses of turnstiles 1–3 are outlined in Scheme 1. First, Sonogashira coupling of 9,10-dibromoanthracene (4) with trimethylsilylacetylene provided 9,10-bis-[(trimethylsilyl)ethynyl]anthracene (6). Benzenediazonium-2-carboxylate 8 prepared from anthranilic acid with isopentyl nitrite was added to the solution of 6 to afford 9,10-bis-[(trimethylsilyl)ethynyl]triptycene (10), followed by depro-

tection with potassium carbonate in the mixtures of methanol and tetrahydrofuran to give 9,10-diethynyltritycenes (**13**).¹⁸ During the synthesis of **18**, we found that 3-ethynylpyridine is too unstable to be isolated at room temperature. Therefore, a one-pot synthetic procedure in which 4-amino-3-iodobenzoic acid ethyl ester (**16**) was coupled with 3-ethynylpyridine generated in situ from 3-[2-(trimethylsilyl)ethynyl]pyridine (**17**) was used to yield compound **18**. Diazotization of **18** in the presence of potassium iodide provided compound **19**. Finally, compound **1** was obtained by palladium-catalyzed cross-coupling of **13** and **19**. Compounds **2** and **3** were synthesized according to the synthetic procedures of **1**. Crystals of **1** obtained by slowly evaporating the solvent mixture of chloroform and acetone at ambient temperature were analyzed by X-ray diffraction and revealed a triclinic system with a space group of $P\bar{1}$ (Figure S1), in which the two pyridyl units of **1** are in the *trans* conformation and may offer enough space for unhindered rotation of the Tp rotor. Compounds **1–3** were characterized by ¹H NMR, ¹³C NMR, ¹H–¹³C HSQC, ¹H–¹³C HMBC, ¹H–¹H NOESY, and HRMS-ESI (see Supporting Information).

¹H NMR Titration. The ¹H NMR spectrum of **1** at 298 K shows only one set of peaks H_b, H_c, and H_d on triptycene, indicating the three phenyl rings on the Tp moiety are chemically equivalent (Figure 2). The data show that the Tp rotor of

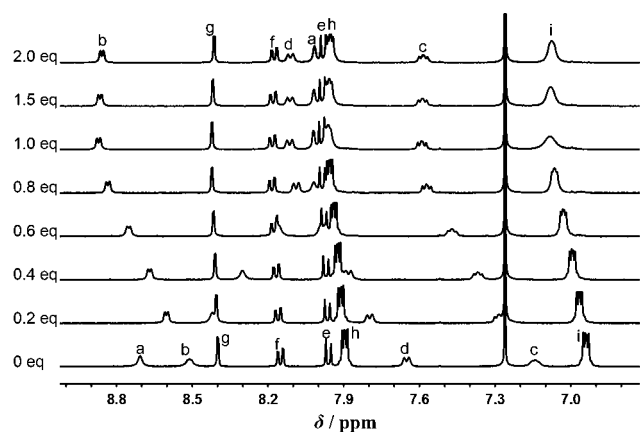


Figure 2. Changes of partial ¹H NMR titration spectra (400 MHz, 298 K) of the molecular turnstile **1** (2 mM) in CDCl₃ upon adding aliquots of AgBF₄ (100 mM) in acetone-*d*₆.

turnstile **1** exhibits an unhindered rotation and the absence of steric interactions between the two stators, implying an open state without silver ions. With the addition of Ag⁺ to the solution of **1**, protons H_b, H_c, and H_d on the pyridyl moieties display significantly downfield shifts with $\Delta\delta$ up to 0.36, 0.45, and 0.46 ppm, respectively. However, proton H_a exhibits a contrary shift with $\Delta\delta$ up to -0.69 ppm. The different tendencies are attributed to the formation of a rigid macrocyclic framework through a linear two-coordinated geometry between pyridyl groups and a silver ion. In such circumstances, protons H_b, H_c, and H_d are located outside the macrocyclic framework, whereas proton H_a is located inside. Moreover, proton H_a is also strongly shielded by the benzene rings on the Tp moiety. No further changes were observed for all protons when the addition of silver ions was greater than 1.0 equiv. The quantitative formation of complex **1Ag** was unambiguously confirmed by ¹H NMR spectroscopy and HRMS-ESI measurement, which shows a peak of *m/z* at 907.17117 for [**1Ag**-BF₄]⁺

(Figure S17). A Job plot for **1** and Ag⁺ shows a maximum at a mole fraction of 0.5 (Figure S4), confirming the 1:1 binding between them. Fitting analyses of the ¹H NMR titration curves gave an association constant (*K*_a) of $2.50 \times 10^4 \text{ M}^{-1}$ ($\Delta G_{298 \text{ K}} = -6.0 \text{ kcal mol}^{-1}$).

The titration ¹H NMR investigations at 298 K revealed the formation of complex **1Ag**. However, protons H_b and H_c on the Tp rotor show slight shifts and no splitting. Lack of shifting and splitting of protons H_b and H_c on the Tp moiety implies a fast exchange regime, which suggests that the steric interactions between the stator and the rotor that originate from metal coordination are not strong enough to halt the rotation of the rotor. The results indicate no detectable closed state under such conditions. In order to achieve readable bistability of the turnstile, we decided to increase the size of the rotor by introducing methyl groups on the phenyl rings of Tp as in our previous report on molecular transmission devices^{12c} to not only enhance the steric interaction between the stator and the rotor in the presence of silver ions but also break the symmetry of the Tp rotor, thus generating different rotamers. Therefore, turnstiles **2** and **3** with different substituents were designed and synthesized accordingly (Scheme 1). Similarly, turnstiles **2** and **3** quantitatively form complexes **2Ag** and **3Ag** with binding constants of $2.50 \times 10^4 \text{ M}^{-1}$ ($\Delta G_{298 \text{ K}} = -6.0 \text{ kcal mol}^{-1}$) and $2.95 \times 10^4 \text{ M}^{-1}$ ($\Delta G_{298 \text{ K}} = -6.1 \text{ kcal mol}^{-1}$), respectively. The ¹H NMR titration experiments reveal that turnstiles **2** and **3** behave similarly to turnstile **1** in the presence of silver ions, but the aromatic protons on triptycenes became broadened with increasing numbers of methyl groups on the Tp rotors at 298 K (Figures S2 and S3), indicating that the substituted methyl groups are able to slightly slow the exchange between the metal complexes and the free ligands due to their steric hindrances. No homomeric rotamers were observed for **2Ag** and **3Ag** (Figures 1 and 4). The data show that the sizes of the rotors exert no effect on the rotation, and the N–Ag–N bond in the macrocyclic framework plays a vital role on restricting the rotation.

Variable-Temperature NMR Experiments of 1–3Ag. In order to shed light on the dynamic exchanged processes of **1–3Ag** complexes, variable-temperature (VT) ¹H NMR experiments were carried out from 298 to 223 K. As shown in Figure 3 and Figures S5–S7 in the Supporting Information, decreasing

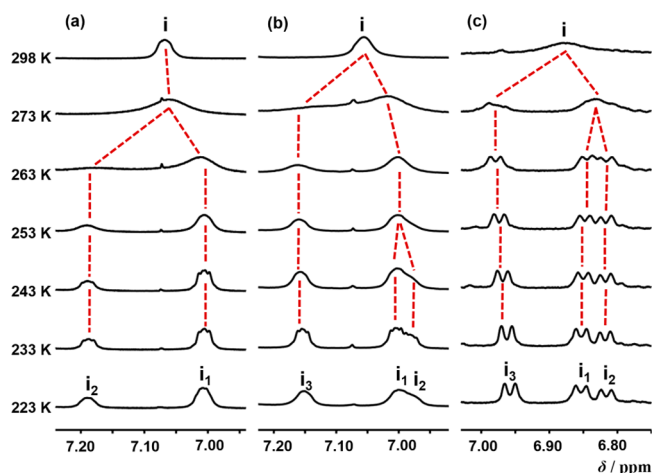


Figure 3. Partial VT ¹H NMR (500 MHz) spectra of proton H_i: (a) **1Ag**, (b) **2Ag**, and (c) **3Ag**. The concentrations of silver complexes are 2 mM in the mixture of CD₃COCD₃/CDCl₃ (1:20 v/v).

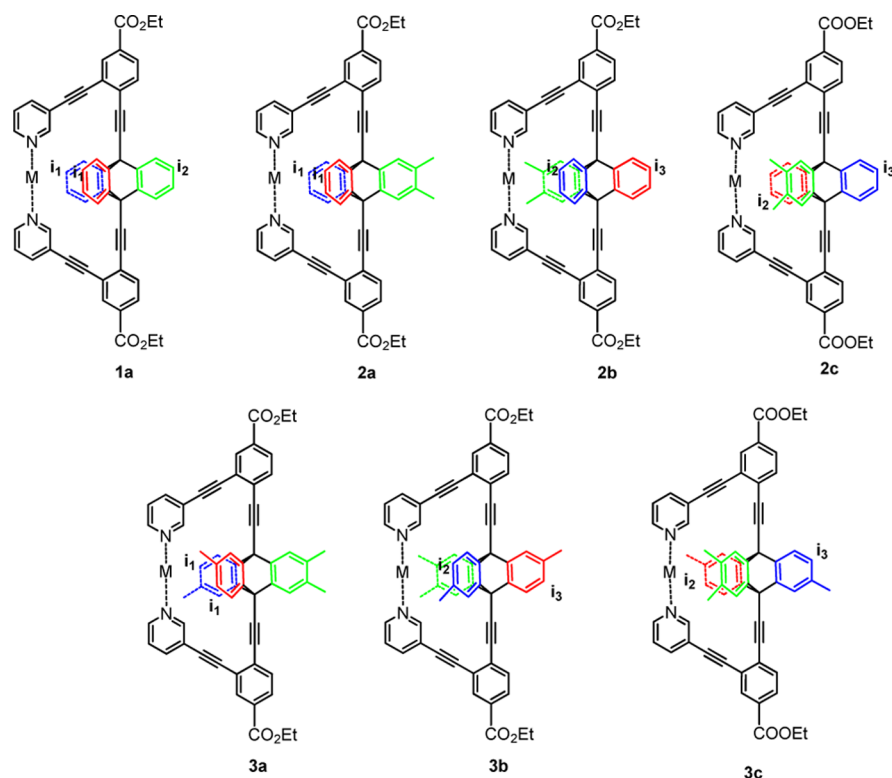


Figure 4. Possible homomeric rotamers of molecular turnstiles in the presence of a metal ion. Complex **1** only has one rotamer (**1a**) because the three phenyl rings on the rotor are chemically identical. Complexes **2** and **3** have three rotamers. Indeed, conformations of **2b/2c** and **3b/3c** are the same because the two phenyl rings on the rotor are chemically identical.

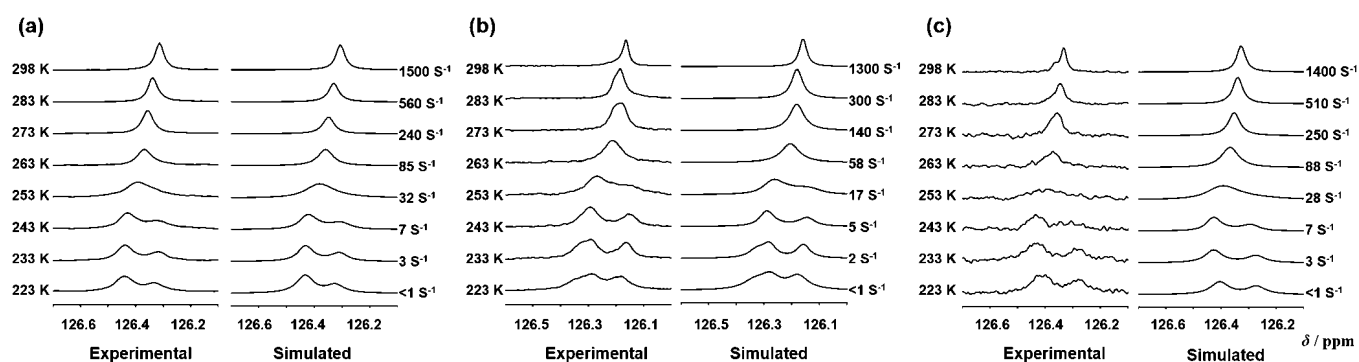


Figure 5. Experiment (left) and simulated (right) VT ^{13}C NMR spectra of carbon C_i : (a) **1Ag**, (b) **2Ag**, and (c) **3Ag** in a mixture of 1:20 (v/v) acetone- d_6 /CDCl $_3$ (500 MHz, [**1Ag**] = [**2Ag**] = 40 mM, [**3Ag**] = 20 mM). The calculated interconversion rate constants (k_v , s^{-1}) are given for each trace. Simulated spectra were performed with the Bruker Topspin 2.1 program.

temperature caused the signals of the protons on triptycene to broaden and then split into two broadened peaks at different temperatures and finally into two or three sharp peaks, with the corresponding ratios in intensity depending on the magnetic properties of the protons and the number of rotamers (Figure 4). For **1Ag**, protons H_i at 7.07 ppm were split into two broadened peaks at 263 K and finally into two sharp peaks, H_{i1} at 7.19 ppm and H_{i2} at 7.01 ppm assigned by NOE at 223 K (Figure S23 and S24) with an intensity ratio of 1:2 (Figures 3a and 4). For **3Ag**, the proton H_i splits into two broadened peaks at 273 K and further into three sharp peaks at 243 K. In this case, one expects three possible homomeric rotamers **3a–c** (Figure 4) due to the differential benzene rings on the triptycyl rotor. Accordingly, protons H_i should display chemical differentials for each rotamer and are denoted accordingly as H_{i1-3} and assigned to the corresponding rotamers by NOE

NMR spectroscopy at 223 K (Figures S25–S28). Since the conformations of rotamers **3b** and **3c** are chemically identical, protons H_{i1-3} appear at 6.96, 6.85, and 6.82 ppm with equal intensities. The effect of temperature on **2Ag** is similar to that for **3Ag** but to a less extent. The results demonstrate that Ag^+ -mediated turnstiles are chemically equivalent at 298 K, exhibiting closed states but are unreadable due to fast exchanges among these different rotamers; when the exchange processes are frozen at low temperature, the closed states are observed.

An attempt to abstract the kinetic parameters for the turnstile complexes by using line shape analysis from variable-temperature ^1H NMR was unsuccessful due to the multiplicity of the aromatic signals. Therefore, we turned to variable temperature ^{13}C NMR spectroscopy. Variable-temperature ^{13}C NMR experiments of complexes **1–3Ag** were performed in a mixture

of CDCl₃ and acetone-*d*₆. The carbons C₁ were monitored in all cases. As shown in Figures 5 and S8–S16, while at 298 K, C₁ displays a single peak around 126.3 ppm and exhibits two peaks with a 2:1 intensity ratio at 223 K for each complex. These findings again support our interpretation that Ag⁺-mediated turnstiles exhibit an unreadable closed state at 298 K due to fast exchanges among rotamers but display a detectable closed state at 223 K as the exchange processes were frozen. The kinetic parameters were obtained by using line shape analysis and are listed in Table 1. To our surprise, the parameters $\Delta G_{298\text{ K}}^{\ddagger}$, ΔH^{\ddagger} ,

Table 1. Summary of the Thermodynamic Parameters for 1Ag, 2Ag, and 3Ag

complex	$\Delta G_{298\text{ K}}^{\ddagger}$ (kcal mol ⁻¹)	ΔH^{\ddagger} (kcal mol ⁻¹)	ΔS^{\ddagger} (cal mol ⁻¹ K ⁻¹)	E_a (kcal mol ⁻¹)
1Ag	13.1 ± 0.9	13.2 ± 0.4	0.5 ± 1.7	13.7 ± 0.4
2Ag	13.2 ± 0.7	13.3 ± 0.3	0.2 ± 1.2	13.8 ± 0.3
3Ag	13.1 ± 1.0	13.1 ± 0.5	0.1 ± 1.8	13.7 ± 0.5

ΔS^{\ddagger} , and E_a of each Ag⁺-mediated turnstile are very close. Similar $\Delta G_{298\text{ K}}^{\ddagger}$ values suggest that the switching process is governed by the binding nature of Ag⁺-coordinated bonds with pyridyl ligands but not by the size of the Tp rotor itself. Large ΔH^{\ddagger} values imply that the switching process is mainly dominated by enthalpy. Interestingly, the change on entropy is small in each case, suggestive of a highly structural integrity during the rotary process.

Calculations. To theoretically illustrate the thermodynamic behaviors of the molecules, the minimum energy profile (MEP) was mapped by intrinsic reaction coordinate (IRC) computation using DFT with the B3LYP hybrid functional and 6-31G* basis set implemented in the Gaussian 03 program package¹⁹ along with the unbiased reaction coordinates to gain insight into how the isomerization of 1Ag (gas phase) takes place. The obtained MEP could be reasonably regarded as the most energetically favorable conformational transformation pathway for the dynamic motion of 1Ag, considering that the molecule has a rigid and shape-persistent macrocyclic framework. The global minimum structure of 1Ag, as shown in Figure 6, possesses a nearly planar macrocyclic frame. Two phenyl rings on the Tp group spatially close to the pyridyl groups are distributed bilaterally and symmetrically to the plane of the macrocycle to accommodate the steric interaction. Complex 1Ag exhibits a continual increase in energy as the Tp moiety rotates due to the increasing steric interactions between the Tp group and the framework, consequently leading to deformation of both of the two silver–pyridine coordination bonds. Proceeding through a transition state (S₀-TS, Figure 6) where both coordination bonds are very weak, one blade of the Tp moiety passes across the quasi-framework fleetly. Notably, the calculations predict that, in this process, the complex prefers to weaken two silver–pyridine bonds rather than cleave one single pyridine–silver bond followed by rotation of the stator arm, which is probably because the latter is more energy-consuming. The complex at the transition state lies ~21 kcal mol⁻¹ higher in energy than the global minimum. This gap is a little larger (~8 kcal mol⁻¹) than the activation energy derived from the VT NMR experiment, which might be ascribed to the presence of solvation-free energies of the ligand and the silver salt in real solution. With the continuous rotation of the blade, the energy gradually decreases. In this process, the silver reassociates with the pyridyl ligands, and finally, a global minimum geometry is

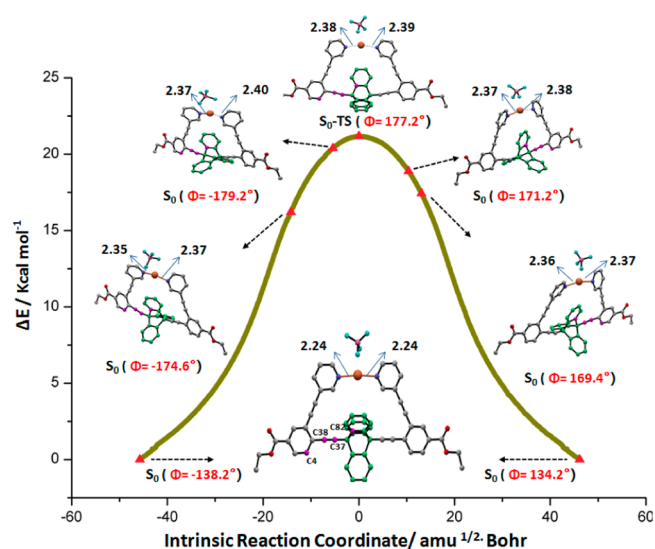


Figure 6. MEP of the conformational transformation pathways of 1Ag, obtained at the DFT//IRC//B3LYP level of theory. The structures at the highlighted characteristic points of the reaction path are given with their C–N distances in angstroms (black) and the dihedral angle (ϕ) of C4–C38(alkyne)–C37(alkyne)–C82 in degrees (red).

reobtained. These results indicate that the dissociation/reassociation of the coordination bond plays a very important role in the rotation in 1Ag, and the fast dissociation/reassociation shows that the macrocyclic framework continues to be rotationally constrained during the whole process, consistent with the phenomenon where little entropy changes could be observed in VT NMR experiments on 1–3Ag.

¹H NMR Experiments of 1–3Pd. In order to circumvent the switching process in Ag⁺-mediated turnstiles at room temperature, a metal ion with a strong affinity to pyridyl ligands is in demand. PdCl₂(CH₃CN)₂ was thus chosen to coordinate pyridyl ligands of the turnstiles due to the fact that a PdCl₂/pyridine complex prefers to adopt a square geometry in which the bonds of Cl–Pd–Cl and N–Pd–N are perpendicular to each other.¹⁶ Pd²⁺-mediated turnstiles were prepared by heating a solution of equal equivalents of compounds 1–3 and PdCl₂(CH₃CN)₂ at 50 °C for 2 h. As expected, the protons of the triptycyl rotor significantly shift downfield and split into multiple peaks at room temperature (Figure 7). For example, for the 1Pd turnstile, protons H_i split into two signals with a 2:1 ratio in intensity. For 2Pd and 3Pd turnstiles, the ¹H NMR spectra show that protons H_i split into three peaks with an equal intensity. The variable-temperature NMR spectra in the range from 298 to 380 K demonstrate that the chemical shifts of the protons on the triptycyl rotors of 1Pd remain constant (Figure S30), supporting the fact that the N–Pd–N bond is very stable. Based on these findings, we concluded that Pd²⁺-mediated turnstiles exhibit a closed state at room temperature, which is significantly different from its Ag⁺-mediated counterparts. DFT calculations show that the energy gap between the palladium complex of 1 in the transition state and that in the energy-minimized conformation is as high as 30 kcal mol⁻¹ (Figure S41), theoretically confirming that the rotation inside 1Pd hardly occurs at ambient temperature.

CONCLUSIONS

In summary, we have designed and synthesized three molecular turnstiles with different sizes of rotors. NMR studies

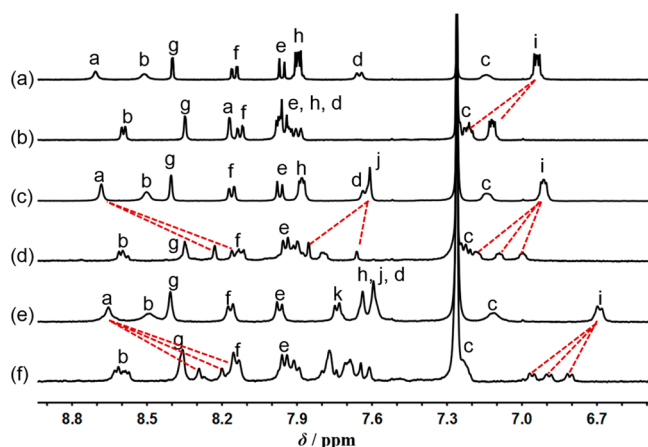


Figure 7. Partial ^1H NMR spectra of **1–3** and the corresponding complexes (400 MHz, 298 K): (a) **1**, (b) **1Pd**, (c) **2**, (d) **2Pd**, (e) **3**, and (f) **3Pd**. The concentrations of the complexes are 2 mM in the mixture of $\text{CD}_3\text{COCD}_3/\text{CDCl}_3$ (1:10 v/v).

demonstrated that the three molecular turnstiles behave in an open state. In the presence of silver ions, the molecular turnstiles behave in a closed state but are unreadable at room temperature. While at low temperature the free rotations among homomeric rotamers were frozen, homomeric rotamers for each case were observed. The turnstiles exhibit as a detectable closed state. In contrast, in the presence of PdCl_2 , the turnstiles show homomeric rotamers and display a detectable closed state at room temperature. The findings support the conclusion that the closed state in the present studies is highly dependent on the binding nature of metal ions to the pyridyl group but independent of the size of the rotor. Our studies provide a new approach to regulate the bistability of molecular turnstiles according to the affinity of metal ions, which is promising for constructing functional molecular devices.

EXPERIMENTAL SECTION

All starting chemicals were obtained from commercial sources and used without further purification. *N,N*-Diisopropylethylamine (*i*- Pr_2NH) and tetrahydrofuran (THF) were distilled over calcium hydride (CaH_2) and sodium benzophenone under an inert atmosphere. Compounds **5**,²⁰ **6**,²¹ **8**,²² **9**,^{12c} **16**,²³ and **17**²⁴ were prepared using procedures reported in the literature. Column chromatography was carried out on flash grade silica gel, using 0–20 psig pressure. NMR spectra were obtained with a 300, 400, and 500 MHz spectrometer using chloroform-*d* (CDCl_3), 1,1,2,2-tetrachloroethane-*d*₂ ($\text{CDCl}_2\text{CDCl}_2$), and acetone-*d*₆ as solvent. The chemical shift references were as follows: (^1H) chloroform-*d*, 7.26 ppm; (^{13}C) chloroform-*d*, 77.16 ppm; (^1H) 1,1,2,2-tetrachloroethane-*d*₂, 6.00 ppm; (^1H) acetone-*d*₆, 2.05 ppm. High-resolution mass spectra (EI, ESI, MALDI) were acquired on GCT, FT-ICR, and MALDI-TOF spectrometers.

2,6-Dimethyl-9,10-bis(trimethylsilyl)ethynylanthracene (7). To a stirred solution of compound **6** (1.82 g, 5 mmol), CuI (0.10 g, 0.5 mmol), and $(\text{Ph}_3\text{P})_2\text{PdCl}_2$ (0.35 g, 0.5 mmol) in diisopropylamine (40 mL) and THF (40 mL) under an argon atmosphere was added trimethylsilylacetylene (2 mL, 15 mmol). The mixture was refluxed for 24 h and then concentrated under reduced pressure. The residue was purified by silica gel column chromatography (petroleum ether (PE)) to give the product as a red solid (1.70 g, 85%): R_f = 0.62 (PE); mp = 206–208 °C; IR (KBr) 3414, 3051, 2914, 2362, 2150, 2123, 1627, 1463, 1369, 1247, 1041, 867, 758, 696, 651, 623, 534 cm^{-1} ; ^1H NMR (400 MHz, CDCl_3) δ = 8.43 (d, J = 8.8 Hz, 2H), 8.28 (s, 2H), 7.43–7.40 (m, 2H), 2.60 (s, 6H), 0.42 (s, 18H); ^{13}C NMR

(100 MHz, CDCl_3) δ = 132.2, 131.2, 129.7, 127.1, 117.3, 107.6, 102.1, 22.3, 0.4; HRMS-ESI (m/z) [$M + \text{H}$]⁺ calcd for $\text{C}_{26}\text{H}_{31}\text{Si}_2$ 399.1964, found 399.1959 (–1.3 ppm).

General Methodology for the Synthesis of Compounds 10–12. Benzynes (**8** or **9**) (7–10 mmol) were added in portions to a mixture of compound **6** or **7** (1 mmol) and 1,2-epoxypropane (2 mL) in dichloroethane (30 mL) and refluxed for 24 h. The reaction mixture was concentrated under reduced pressure. The resultant solid was washed with methanol, and the residue was purified by silica gel column chromatography.

9,10-Bis(trimethylsilyl)ethynyltriptycene (10). Purification by silica gel column chromatography (PE) gave compound **10** as a white solid (195 mg, 42%): R_f = 0.55 (PE); mp = 228–229 °C; IR (KBr) 3441, 3069, 2957, 2183, 1607, 1454, 1303, 1251, 1045, 834, 752, 638, 617, 488 cm^{-1} ; ^1H NMR (400 MHz, CDCl_3) δ = 7.70–7.72 (m, 6H), 7.08–7.10 (m, 6H), 0.46 (s, 18H); ^{13}C NMR (100 MHz, CDCl_3) δ = 143.5, 125.9, 122.4, 99.8, 98.3, 53.2, 0.5; HRMS-MALDI (m/z) [$M + \text{Na}$]⁺ calcd for $\text{C}_{30}\text{H}_{30}\text{NaSi}_2$ 469.1778, found 469.1782 (–0.7 ppm).

2,3-Dimethyl-9,10-bis(trimethylsilyl)ethynyltriptycene (11). Purification by silica gel column chromatography (PE) gave compound **11** as a white solid (150 mg, 32%): R_f = 0.53 (PE); mp = 241–243 °C; IR (KBr) 3415, 3067, 2954, 2897, 2182, 1452, 1296, 1249, 1229, 1163, 1067, 1020, 854, 760, 744, 640, 486 cm^{-1} ; ^1H NMR (400 MHz, CDCl_3) δ = 7.67–7.69 (m, 4H), 7.46 (s, 2H), 7.06–7.08 (m, 4H), 2.19 (s, 6H), 0.46 (s, 18H); ^{13}C NMR (100 MHz, CDCl_3) δ = 143.6, 140.7, 135.5, 126.1, 125.8, 123.2, 122.2, 122.1, 100.2, 98.0, 52.7, 21.4, 0.5; HRMS-MALDI (m/z) [$M + \text{Na}$]⁺ calcd for $\text{C}_{32}\text{H}_{34}\text{NaSi}_2$ 497.2091, found 497.2095 (–0.8 ppm).

2,3,6,14-Tetramethyl-9,10-bis(trimethylsilyl)ethynyl-triptycene (12). Purification by silica gel column chromatography (PE) gave compound **12** as a white solid (75 mg, 15%): R_f = 0.52 (PE); mp = 267–268 °C; IR (KBr) 3421, 2959, 2920, 2360, 2178, 1609, 1466, 1250, 1157, 1020, 844, 758, 623, 486 cm^{-1} ; ^1H NMR (400 MHz, CDCl_3) δ = 7.52 (d, J = 7.2 Hz, 2H), 7.48 (s, 2H), 7.43 (s, 2H), 6.84 (d, J = 7.6 Hz, 2H), 2.27 (s, 6H), 2.18 (s, 6H), 0.46 (s, 18H); ^{13}C NMR (100 MHz, CDCl_3) δ = 141.2, 140.9, 135.4, 133.6, 125.6, 123.6, 123.0, 121.9, 100.5, 97.7, 52.3, 21.3, 19.8, 0.5; HRMS-MALDI (m/z) [$M + \text{Na}$]⁺ calcd for $\text{C}_{34}\text{H}_{38}\text{NaSi}_2$ 525.2404, found 525.2410 (1.1 ppm).

General Methodology for the Synthesis of Compounds 13–15. A mixture of starting material (**10**, **11**, or **12**, 1 mmol) and K_2CO_3 (4 mmol) in 1:1 (v/v) methanol/THF was stirred at room temperature for 16 h. After all solvent was removed under reduced pressure, water was added to the residue and the aqueous phase was extracted with CH_2Cl_2 (three times). The combined organic phase was dried with anhydrous MgSO_4 and concentrated to afford the corresponding products **13–15**.

9,10-Diethynyltriptycene (13). Compound **13** was obtained as a white solid (278 mg, 92%): R_f = 0.48 (PE); mp = 279–281 °C; IR (KBr) 3412, 3284, 2922, 2360, 1607, 1454, 1303, 1032, 878, 748, 638, 490, 430 cm^{-1} ; ^1H NMR (400 MHz, CDCl_3) δ = 7.75–7.77 (m, 6H), 7.10–7.12 (m, 6H), 3.30 (s, 2H); ^{13}C NMR (100 MHz, CDCl_3) δ = 143.1, 126.0, 122.3, 81.1, 78.2, 53.4; HRMS-EI (m/z) [M]⁺ calcd for $\text{C}_{24}\text{H}_{14}$ 302.1096, found 302.1092 (–1.2 ppm).

2,3-Dimethyl-9,10-diethynyltriptycene (14). Compound **14** was obtained as a white solid (300 mg, 91%): R_f = 0.45 (PE); mp = 254–256 °C; IR (KBr) 3468, 3373, 3305, 2361, 1707, 1654, 1458, 862, 758, 654 cm^{-1} ; ^1H NMR (400 MHz, CDCl_3) δ = 7.58 (d, J = 7.6 Hz, 2H), 7.53 (s, 2H), 7.48 (s, 2H), 6.86 (d, J = 7.2 Hz, 2H), 3.27 (s, 2H), 2.28 (s, 6H), 2.19 (s, 6H); ^{13}C NMR (100 MHz, CDCl_3) δ = 140.9, 140.7, 135.6, 123.8, 126.1, 123.6, 122.9, 121.9, 80.6, 78.7, 51.5, 21.3, 19.6; HRMS-EI (m/z) [M]⁺ calcd for $\text{C}_{26}\text{H}_{18}$ 330.1409, found 330.1406 (–0.8 ppm).

2,3,6,14-Tetramethyl-9,10-diethynyltriptycene (15). Compound **15** was obtained as a white solid (322 mg, 90%): R_f = 0.42 (PE); mp = 229–230 °C; IR (KBr) 3421, 3330, 2854, 2345, 1607, 1463, 1298, 1134, 1034, 881, 850, 825, 671, 656 cm^{-1} ; ^1H NMR (400 MHz, CDCl_3) δ = 7.58 (d, J = 7.6 Hz, 2H), 7.53 (s, 2H), 7.48 (s, 2H), 6.86 (d, J = 7.3 Hz, 2H), 3.27 (t, J = 12 Hz, 2H), 2.28 (s, 6H), 2.19 (s, 6H); ^{13}C NMR (100 MHz, CDCl_3) δ = 143.3, 140.6, 134.0, 125.9,

123.7, 122.1, 80.8, 78.4, 51.9, 19.6; HRMS-EI (m/z) [M]⁺ calcd for C₂₈H₂₂ 358.1722, found 358.1726 (1.3 ppm).

4-Amino-3-(pyridin-3-ylethynyl)benzoic Acid Ethyl Ester (18). The mixture of **16** (0.29 g, 1 mmol), **17** (0.18 g, 1 mmol), tetrabutylammonium fluoride (TBAF, 0.16 g, 0.5 mmol), CuI (0.04 g, 0.2 mmol), and (Ph₃P)₂PdCl₂ (0.07 g, 0.1 mmol) in diisopropylamine (10 mL) and THF (20 mL) was refluxed for 24 h at 70 °C under an argon atmosphere. The filtrate was evaporated under reduced pressure and purified by silica gel column chromatography (eluant: CH₂Cl₂/ethyl acetate = 200:1) to give the product as a white solid (0.22 g, 82%); R_f = 0.55 (CH₂Cl₂/ethyl acetate, 4/1); mp = 136–138 °C; IR (KBr) 3431, 3327, 3190, 2355, 2203, 1692, 1628, 1602, 1504, 1471, 1433, 1344, 1279, 1246, 1144, 1024, 833, 767, 702, 629 cm⁻¹; ¹H NMR (400 MHz, CDCl₃) δ = 8.77 (d, J = 1.6 Hz, 1H), 8.57 (dd, J = 5.2, 1.6 Hz, 1H), 8.10 (d, J = 2.0 Hz, 1H), 7.85 (dd, J = 8.4, 1.6 Hz, 1H), 7.81 (td, J = 8.0, 1.6 Hz, 1H), 7.28–7.32 (m, 1H), 6.72 (d, J = 8.4 Hz, 1H), 4.69 (br, 2H), 4.33 (q, J = 7.2 Hz, 2H), 1.38 (t, J = 7.2 Hz, 3H); ¹³C NMR (100 MHz, CDCl₃) δ = 166.1, 152.1, 151.7, 148.8, 138.4, 134.6, 132.0, 123.2, 120.2, 119.8, 113.5, 106.2, 91.5, 88.4, 60.6, 14.5; HRMS-ESI (m/z) [M + H]⁺ calcd for C₁₆H₁₅N₂O₂ 267.1134, found 267.1136 (0.7 ppm).

4-Iodo-3-(pyridin-3-ylethynyl)benzoic Acid Ethyl Ester (19). A solution of NaNO₂ (0.69 g, 10 mmol) in water (3 mL) was added dropwise to a mixture of compound **18** (1.0 g, 4 mmol) in water (15 mL) and concentrated hydrochloric acid (5 mL) at 5 °C. The mixture was stirred for 30 min, and a solution of potassium iodide (1.2 g, 10 mmol) in water (3 mL) was added. The mixture was stirred for 15 min below 5 °C and then at room temperature for 1 h. After that, the mixture was cooled to 0 °C, and a solution of 5% aqueous sodium sulfite (10 mL) was added. The organic layer was separated, and the water layer was extracted with CH₂Cl₂ (30 mL, three times). The combined organic phases were dried over Na₂SO₄. After removal of the solvents under reduced pressure, the crude product was purified by column chromatography (eluant: CH₂Cl₂/ethyl acetate = 200:1) to give the product as a white solid (1.0 g, 66%); R_f = 0.42 (CH₂Cl₂/ethyl acetate, 4/1); mp = 132–133 °C; IR (KBr) 3436, 3329, 3197, 2358, 2328, 1712, 1477, 1409, 1278, 1238, 1159, 1101, 1018, 758, 418 cm⁻¹; ¹H NMR (400 MHz, CDCl₃) δ = 8.89 (s, 1H), 8.64 (s, 1H), 8.17 (d, J = 2.0 Hz, 1H), 7.98 (d, J = 8.4 Hz, 1H), 7.88 (d, J = 8.0 Hz, 1H), 7.67 (dd, J = 8.0, 2.0 Hz, 1H), 7.34 (s, 1H), 4.39 (q, J = 7.2 Hz, 2H), 1.41 (t, J = 7.2 Hz, 3H); ¹³C NMR (100 MHz, CDCl₃) δ = 165.5, 152.3, 149.2, 139.2, 138.6, 133.3, 130.7, 130.4, 129.7, 123.4, 107.0, 94.0, 90.5, 61.6, 14.4; HRMS-ESI (m/z) [M + H]⁺ calcd for C₁₆H₁₃INO₂ 377.9991, found 377.9987 (−1.1 ppm).

General Methodology for the Synthesis of Compounds 1–3.

The mixture of compound **13**, **14**, or **15** (1.0 equiv), **19** (2.0 equiv), CuI (0.2 equiv), and (Ph₃P)₂PdCl₂ (0.1 equiv) in diisopropylamine and THF was stirred overnight under an argon atmosphere. The filtrate was evaporated under reduced pressure, and the residue was purified by silica gel column chromatography to afford the corresponding products **1–3**.

Compound 1. Purification by silica gel column chromatography (eluant: CH₂Cl₂/CH₃OH = 200:1) gave compound **1** in 50% yield as a white solid; R_f = 0.72 (CH₂Cl₂/CH₃OH, 30/1); mp = 257–259 °C; IR (KBr) 3454, 2982, 1720, 1454, 1415, 1263, 1242, 1155, 1111, 1022, 937, 758, 638, 420 cm⁻¹; ¹H NMR (400 MHz, CDCl₃) δ = 8.71 (s, 2H), 8.51 (d, J = 4.0 Hz, 2H), 8.39 (d, J = 1.6 Hz, 2H), 8.14 (dd, J = 8.4, 2.0 Hz, 2H), 7.95 (d, J = 8.4 Hz, 2H), 7.88–7.91 (m, 5H), 7.63 (d, J = 8.0 Hz, 2H), 7.11 (t, J = 7.6 Hz, 2H), 6.92–6.96 (m, 5H), 4.47 (q, J = 7.2 Hz, 2H), 1.47 (t, J = 7.2 Hz, 3H); ¹³C NMR (100 MHz, CDCl₃) δ = 165.4, 152.4, 149.1, 143.3, 138.9, 133.6, 132.9, 130.7, 129.6, 129.4, 126.1, 125.8, 122.5, 91.1, 90.9, 90.8, 61.7, 53.3, 14.5; HRMS-ESI (m/z) [M + H]⁺ calcd for C₅₆H₃₇N₂O₄ 801.2753, found 801.2766 (1.6 ppm).

Compound 2. Purification by silica gel column chromatography (eluant: CH₂Cl₂/CH₃OH = 200:1) gave compound **2** in 37% yield as a white solid; R_f = 0.68 (CH₂Cl₂/CH₃OH, 30/1); mp = 253–255 °C; IR (KBr) 3470, 2922, 2851, 2376, 1719, 1420, 1265, 1155, 1130, 1020, 766, 700, 623, 418 cm⁻¹; ¹H NMR (400 MHz, CDCl₃) δ = 8.70 (d, J = 1.2 Hz, 2H), 8.48 (d, J = 4.8 Hz, 2H), 8.40 (d, J = 1.6 Hz, 2H), 8.14

(dd, J = 8.4, 2.0 Hz, 2H), 7.96 (d, J = 8.4 Hz, 2H), 7.87–7.89 (m, 4H), 7.59–7.60 (m, 4H), 7.09 (dd, J = 7.8, 4.8 Hz, 2H), 6.89–6.91 (m, 4H), 4.47 (q, J = 7.2 Hz, 2H), 1.47 (t, J = 7.2 Hz, 3H); ¹³C NMR (100 MHz, CDCl₃) δ = 165.8, 152.4, 149.0, 143.6, 140.8, 139.1, 134.1, 133.6, 132.9, 130.7, 129.6, 126.0, 125.9, 123.9, 123.1, 122.4, 119.9, 91.3, 91.0, 91.0, 90.9, 61.7, 52.9, 19.6, 14.5; HRMS-ESI (m/z) [M + H]⁺ calcd for C₅₈H₄₁N₂O₄ 829.3066, found 829.3052 (−1.7 ppm).

Compound 3. Purification by silica gel column chromatography (eluant: CH₂Cl₂/CH₃OH = 200:1) gave compound **3** in 30% yield as a white solid; R_f = 0.65 (CH₂Cl₂/CH₃OH, 30/1); mp = 253–255 °C; IR (KBr) 3354, 2978, 2362, 1718, 1600, 1466, 1416, 1256, 1155, 1111, 1095, 1022, 804, 764 cm⁻¹; ¹H NMR (400 MHz, CDCl₃) δ = 8.67 (s, 2H), 8.47 (s, 2H), 8.40 (d, J = 1.2 Hz, 2H), 8.15 (dd, J = 8.0, 1.6 Hz, 2H), 7.96 (d, J = 8.0 Hz, 2H), 7.74 (d, J = 7.6 Hz, 2H), 7.64 (d, J = 5.2 Hz, 2H), 7.55–7.61 (m, 4H), 7.05 (s, 2H), 6.67 (s, J = 6.8 Hz, 2H), 4.47 (q, J = 7.2 Hz, 2H), 1.47 (t, J = 7.2 Hz, 3H); ¹³C NMR (100 MHz, CDCl₃) δ = 165.5, 152.4, 149.0, 143.8, 141.1, 140.9, 139.0, 135.7, 135.6, 133.9, 133.5, 132.9, 130.6, 129.7, 129.6, 126.2, 125.9, 123.7, 123.1, 122.2, 119.9, 91.7, 91.0, 90.7, 61.7, 52.5, 21.2, 19.5, 14.5; HRMS-ESI (m/z) [M + H]⁺ calcd for C₆₀H₄₅N₂O₄ 857.3379, found 857.3367 (−1.4 ppm).

■ ASSOCIATED CONTENT

Supporting Information

The Supporting Information is available free of charge on the ACS Publications website at DOI: 10.1021/acs.joc.6b00463.

VT NMR spectra and Eyring plot analyses of **1–3Ag**; computational details; and ¹H, ¹³C, and 2D NMR spectra (PDF)

X-ray data of **1** (CIF)

■ AUTHOR INFORMATION

Corresponding Authors

*E-mail: ywangl@bnu.edu.cn

*E-mail: xuebochen@bnu.edu.cn.

*E-mail: ykche@iccas.ac.cn.

*E-mail: jiangh@bnu.edu.cn.

Notes

The authors declare no competing financial interest.

■ ACKNOWLEDGMENTS

This work was supported by the National Natural Science Foundation of China (21125205, 21332008, 21472015, and 21572023), the 973 Program (2015CB856502), the Youth Scholars Program of Beijing Normal University (2014NT08), and the Fundamental Research Funds for the Central Universities.

■ REFERENCES

- (a) Balzani, V.; Credi, A.; Raymo, F. M.; Stoddart, J. F. *Angew. Chem., Int. Ed.* **2000**, *39*, 3348–3391. (b) Kottas, G. S.; Clarke, L. I.; Horinek, D.; Michl, J. *Chem. Rev.* **2005**, *105*, 1281–1376. (c) Kinbara, K.; Aida, T. *Chem. Rev.* **2005**, *105*, 1377–1400. (d) Kay, E. R.; Leigh, D. A.; Zerbetto, F. *Angew. Chem., Int. Ed.* **2007**, *46*, 72–191. (e) Ma, X.; Tian, H. *Chem. Soc. Rev.* **2010**, *39*, 70–80.
- (a) Anelli, P. L.; Spencer, N.; Stoddart, J. F. *J. Am. Chem. Soc.* **1991**, *113*, 5131–5133. (b) Sauvage, J. P. *Science* **2001**, *291*, 2105–2106. (c) Keaveney, C. M.; Leigh, D. A. *Angew. Chem., Int. Ed.* **2004**, *43*, 1222–1224. (d) Young, P. G.; Hirose, K.; Tobe, Y. *J. Am. Chem. Soc.* **2014**, *136*, 7899–7906. (e) Young, P. G.; Hirose, K.; Tobe, Y. *J. Am. Chem. Soc.* **2014**, *136*, 7899–7906. (f) Zhu, K.; O’Keefe, C. A.; Vukotic, V. N.; Schurko, R. W.; Loeb, S. J. *Nat. Chem.* **2015**, *7*, 514–519.
- (a) Leigh, D. A.; Wong, J. K. Y.; Dehez, F.; Zerbetto, F. *Nature* **2003**, *424*, 174–179. (b) Fletcher, S. P.; Dumur, F.; Pollard, M. M.;

- Feringa, B. L. *Science* **2005**, *310*, 80–82. (c) Hiraoka, S.; Hisanaga, Y.; Shiro, M.; Shionoya, M. *Angew. Chem., Int. Ed.* **2010**, *49*, 1669–1673.
- (4) (a) Pramanik, S.; De, S.; Schmittel, M. *Angew. Chem., Int. Ed.* **2014**, *53*, 4709–4713. (b) De, S.; Pramanik, S.; Schmittel, M. *Angew. Chem., Int. Ed.* **2014**, *53*, 14255–14259. (c) Bléger, D.; Hecht, S. *Angew. Chem., Int. Ed.* **2015**, *54*, 11338–11349. (d) Tietze, L. F.; Waldecker, B.; Ganapathy, D.; Eichhorst, C.; Lenzer, T. K. O.; Reichmann, S. O.; Stalke, D. *Angew. Chem., Int. Ed.* **2015**, *54*, 10317–10321.
- (5) (a) Dominguez, Z.; Dang, H.; Strouse, M. J.; Garcia-Garibay, M. A. *J. Am. Chem. Soc.* **2002**, *124*, 2398–2399. (b) Gould, S. L.; Tranchemontagne, D.; Yaghi, O. M.; Garcia-Garibay, M. A. *J. Am. Chem. Soc.* **2008**, *130*, 3246–3247. (c) Commins, P.; Garcia-Garibay, M. A. *J. Org. Chem.* **2014**, *79*, 1611–1619. (d) Shima, T.; Hampel, F.; Gladysz, J. A. *Angew. Chem., Int. Ed.* **2004**, *43*, 5537–5540. (e) Setaka, W.; Yamaguchi, K. *J. Am. Chem. Soc.* **2012**, *134*, 12458–1246. (f) Nawara, A. J.; Shima, T.; Hampel, F.; Gladysz, J. A. *J. Am. Chem. Soc.* **2006**, *128*, 4962–4963.
- (6) (a) Bedard, T. C.; Moore, J. S. *J. Am. Chem. Soc.* **1995**, *117*, 10662–10671. (b) Hirata, O.; Takeuchi, M.; Shinkai, S. *Chem. Commun.* **2005**, 3805–3807. (c) Zhou, Z. C.; Zhang, X.; Liu, Q. H.; Yan, Z. Q.; Lv, C. J.; Long, G. *Inorg. Chem.* **2013**, *52*, 10258–10263.
- (7) (a) Wang, J. B.; Feringa, B. L. *Science* **2011**, *331*, 1429–1432. (b) Lewandowski, B.; De Bo, G.; Ward, J. W.; Papmeyer, M.; Kuschel, S.; Aldegunde, M. J.; Gramlich, P. M. E.; Heckmann, D.; Goldup, S. M.; D'Souza, D. M.; Fernandes, A. E.; Leigh, D. A. *Science* **2013**, *339*, 189–193. (c) Blanco, V.; Leigh, D. A.; Lewandowska, U.; Lewandowski, B.; Marcos, V. J. *J. Am. Chem. Soc.* **2014**, *136*, 15775–15780.
- (8) (a) Guenet, A.; Graf, E.; Kyrtsakas, N.; Hosseini, M. W. *Inorg. Chem.* **2010**, *49*, 1872–1883. (b) Lang, T.; Graf, E.; Kyrtsakas, N.; Hosseini, M. W. *Dalton Trans.* **2011**, *40*, 3517–3523. (c) Lang, T.; Graf, E.; Kyrtsakas, N.; Hosseini, M. W. *Dalton Trans.* **2011**, *40*, 5244–5248. (d) Lang, T.; Graf, E.; Kyrtsakas, N.; Hosseini, M. W. *Chem. - Eur. J.* **2012**, *18*, 10419–10426. (e) Zigon, N.; Guenet, A.; Graf, E.; Hosseini, M. W. *Chem. Commun.* **2013**, *49*, 3637–3639. (f) Zigon, N.; Hosseini, M. W. *Chem. Commun.* **2015**, *51*, 12486–12489.
- (9) (a) Hiraoka, S.; Hirata, K.; Shionoya, M. *Angew. Chem., Int. Ed.* **2004**, *43*, 3814–3818. (b) Hiraoka, S.; Shiro, M.; Shionoya, M. *J. Am. Chem. Soc.* **2004**, *126*, 1214–1218.
- (10) (a) Albrecht, M. *Chem. Rev.* **2001**, *101*, 3457–3497. (b) Dong, Z.; Yap, G. P. A.; Fox, J. M. *J. Am. Chem. Soc.* **2007**, *129*, 11850–11853. (c) Li, Q. L.; Huang, F.; Fan, Y. X.; Wang, Y. L.; Li, J. F.; He, Y. J.; Jiang, H. *Eur. J. Inorg. Chem.* **2014**, *2014*, 3235–3244.
- (11) (a) Yoshizawa, M.; Takeyama, Y.; Okano, T.; Fujita, M. *J. Am. Chem. Soc.* **2003**, *125*, 3243–3247. (b) Hiraoka, S.; Harano, K.; Shiro, M.; Shionoya, M. *Angew. Chem., Int. Ed.* **2005**, *44*, 2727–2731. (c) Kishi, N.; Akita, M.; Kamiya, M.; Hayashi, S.; Hsu, H. F.; Yoshizawa, M. *J. Am. Chem. Soc.* **2013**, *135*, 12976–12979. (d) Brown, C. J.; Toste, F. D.; Bergman, R. G.; Raymond, K. N. *Chem. Rev.* **2015**, *115*, 3012–3035. (e) Gan, Q.; Ronson, T. K.; Vosburg, D. A.; Thoburn, J. D.; Nitschke, J. R. *J. Am. Chem. Soc.* **2015**, *137*, 1770–1773.
- (12) (a) Gan, Q.; Ferrand, Y.; Bao, C. Y.; Kauffmann, B.; Grélard, A.; Jiang, H.; Huc, I. *Science* **2011**, *331*, 1172–1175. (b) Wang, G. X.; Che, Y. K.; Jiang, H. *Progress in Chemistry* **2014**, *26*, 909–918. (c) Wang, G. X.; Ma, L. S.; Xiang, J. F.; Wang, Y.; Chen, X. B.; Che, Y. K.; Jiang, H. *J. Org. Chem.* **2015**, *80*, 11302–11312.
- (13) (a) Iwamura, H.; Mislow, K. *Acc. Chem. Res.* **1988**, *21*, 175–182. (b) Kao, C. Y.; Hsu, Y. T.; Lu, H. F.; Chao, I.; Huang, S. L.; Lin, Y. C.; Sun, W. T.; Yang, J. S. *J. Org. Chem.* **2011**, *76*, 5782–5792.
- (14) (a) Kelly, T. R.; Bowyer, M. C.; Bhaskar, K. V.; Bebbington, D.; Garcia, A.; Lang, F.; Kim, M. H.; Jette, M. P. *J. Am. Chem. Soc.* **1994**, *116*, 3657–3658. (b) Yang, J. S.; Huang, Y. H.; Ho, J. H.; Sun, W. T.; Huang, H. H.; Lin, Y. C.; Huang, S. J.; Huang, S. L.; Lu, H. F.; Chao, I. *Org. Lett.* **2008**, *10*, 2279–2282.
- (15) Annunziata, R.; Benaglia, M.; Cinquini, M.; Raimondi, L.; Cozzi, F. *J. Phys. Org. Chem.* **2004**, *17*, 749–751.
- (16) (a) Meng, Z.; Xiang, J. F.; Chen, C. F. *Chem. Sci.* **2014**, *5*, 1520–1525. (b) Meng, Z.; Han, Y.; Wang, L. N.; Xiang, J. F.; He, S. G.; Chen, C. F. *J. Am. Chem. Soc.* **2015**, *137*, 9739–9745.
- (17) (a) Stone, M. T.; Moore, J. S. *J. Am. Chem. Soc.* **2005**, *127*, 5928–5935. (b) Ren, Q. W.; Reedy, C. G.; Terrell, E. A.; Wieting, J. M.; Wagie, R. W.; Asplin, J. P.; Doyle, L. M.; Long, S. J.; Everard, M. T.; Sauer, J. S.; Baumgart, C. E.; D'Acchioli, J. S.; Bowling, N. P. *J. Org. Chem.* **2012**, *77*, 2571–2577. (c) Hamm, D. C.; Braun, L. A.; Burazin, A. N.; Gauthier, A. M.; Ness, K. O.; Biebel, C. E.; Sauer, J. S.; Tanke, R.; Noll, B. C.; Bosch, E.; Bowling, N. P. *Dalton Trans.* **2013**, *42*, 948–958.
- (18) Caskey, D. C.; Wang, B.; Zheng, X. L.; Michl, J. *Collect. Czech. Chem. Commun.* **2005**, *70*, 1970–1985.
- (19) Frisch, M. J.; Trucks, G. W.; Schlegel, H. B.; Scuseria, G. E.; Robb, M. A.; Cheeseman, J. R.; Montgomery, J. A., Jr.; Vreven, T.; Kudin, K. N.; Burant, J. C.; Millam, J. M.; Iyengar, S. S.; Tomasi, J.; Barone, V.; Mennucci, B.; Cossi, M.; Scalmani, G.; Rega, N.; Petersson, G. A.; Nakatsuji, H.; Hada, M.; Ehara, M.; Toyota, K.; Fukuda, R.; Hasegawa, J.; Ishida, M.; Nakajima, T.; Honda, Y.; Kitao, O.; Nakai, H.; Klene, M.; Li, X.; Knox, J. E.; Hratchian, H. P.; Cross, J. B.; Adamo, C.; Jaramillo, J.; Gomperts, R.; Stratmann, R. E.; Yazyev, O.; Austin, A. J.; Cammi, R.; Pomelli, C.; Ochterski, J. W.; Ayala, P. Y.; Morokuma, K.; Voth, G. A.; Salvador, P.; Dannenberg, J. J.; Zakrzewski, V. G.; Dapprich, S.; Daniels, A. D.; Strain, M. C.; Farkas, O.; Malick, D. K.; Rabuck, A. D.; Raghavachari, K.; Foresman, J. B.; Ortiz, J. V.; Cui, Q.; Baboul, A. G.; Clifford, S.; Cioslowski, J.; Stefanov, B. B.; Liu, G.; Liashenko, A.; Piskorz, P.; Komaromi, I.; Martin, R. L.; Fox, D. J.; Keith, T.; Al-Laham, M. A.; Peng, C. Y.; Nanayakkara, A.; Challacombe, M.; Gill, P. M. W.; Johnson, B.; Chen, W.; Wong, M. W.; Gonzalez, C.; Pople, J. A. *Gaussian 03*, revision D.02; Gaussian, Inc.: Pittsburgh, PA, 2004.
- (20) Xu, J.; Fang, Y. J.; Ren, P. H.; Zhang, H. C.; Guo, E. Q.; Yang, W. J. *Macromol. Rapid Commun.* **2008**, *29*, 1415–1420.
- (21) Ou, Y. P.; Jiang, C. Y.; Wu, D.; Xia, J. L.; Yin, J.; Jin, S.; Yu, G. A.; Liu, S. H. *Organometallics* **2011**, *30*, 5763–5770.
- (22) Klanderma, B. H.; Criswell, T. R. *J. Org. Chem.* **1969**, *34*, 3426–3430.
- (23) Jones, T. V.; Slutsky, M. M.; Laos, R.; de Greef, T. F. A.; Tew, G. N. *J. Am. Chem. Soc.* **2005**, *127*, 17235–17240.
- (24) Holmes, B. T.; Pennington, W. T.; Hanks, T. W. *Synth. Commun.* **2003**, *33*, 2447–2461.